Secular Variation of Iron Isotopes in North Atlantic Deep Water

Xiang-Kun Zhu,* R. Keith O'Nions, Yueling Guo, Ben C. Reynolds

A high-precision iron isotope time series for a ferromanganese crust demonstrates that the iron isotope composition in North Atlantic Deep Water has changed substantially over the past 6 million years and that iron isotope variations in the crust are closely correlated to those of lead isotopes. The close correlation between the two isotope series indicates that the observed iron isotope variations predominantly reflect those of iron input from terrigenous sources and provides no evidence for biologically induced mass fractionation within North Atlantic Deep Water.

The study of natural variations in stable isotope abundance over the years has had a profound influence in many research fields ranging from the life and biomedical sciences to planetary, Earth, and environmental sciences. As one of the most abundant elements in the solar system and as a redox element that has been biologically utilized since the early beginnings of life, Fe is a particularly interesting target for stable isotope measurement. However, investigation of the potential offered by Fe isotopes has been hampered, until very recently, by the absence of suitable techniques for precise Fe isotope ratio measurements (*1–3*). The isotope composition of Fe in seawater is an important issue because Fe plays a controlling role in biological productivity in the oceans (*4–8*) and its abundance in seawater may have a substantial effect on climate changes (*9*). Whereas direct measurement of the isotopic composition of dissolved Fe in seawater is not feasible at present (*10*), hydrogenous ferromanganese (Fe-Mn) crusts have provided excellent records of isotope compositions of other dissolved metals in deep seawater (*11–13*). Thus, in principle, spatial or temporal variations of Fe isotopes in the oceans may be reconstructed from Fe-Mn crusts. Here, we report the results of high-precision Fe isotope measurements of a Fe-Mn crust from the North Atlantic, using the recently developed technique of multiple collector inductively coupled plasma source mass spectrometry (MC-ICPMS) (*1*).

The Fe-Mn crust selected for this study is sample BM1969.05, dredged from the San Pablo seamount at 1829-m depth in the northwest Atlantic (39°0′N, 60°57′W). This crust has been the subject of detailed studies on Pb and Nd isotopes (*14–16*), and its growth rate has been estimated at 1.62 mm per million years (My) with the $^{10}Be/^{9}Be$ method (*15*). Iron isotope analyses were performed on a subset of sample aliquots taken for a high-resolution Pb isotope profile of the crust (*16*). The crust was sampled continuously at a high spatial resolution on a computer-controlled milling machine with a drill depth resolution of ±0.005 mm to produce a typical sample size of ~10 mg. Iron isotope analyses of the samples were carried out by MC-ICPMS after chemical purification (*17*). Analogous to the formalism adopted for high-precision measurements of Cu isotopes (*18*), measured $^{57}Fe/^{54}Fe$ ratios are expressed in terms of $\varepsilon^{57}Fe$ units, which are deviations in parts per 10^4 from the Fe isotope reference standard IRMM-14 (*19*). The Fe isotope results are presented in Web table 1 (available at www.sciencemag.org/feature/data/1046486.shl) together with the corresponding age estimates and Pb isotope data for the analyzed crust. Also, presented in Web table 2 (also available at www.sciencemag.org/feature/data/1046486.shl) are Fe isotope measurements on six iron meteorites and four samples of Chinese loess. These results serve as references for the isotope compositions of Fe in the solar system and the upper continental crust.

The Fe isotopes from the Fe-Mn crust have an overall variation of ~14 $\varepsilon^{57}Fe$ units with $-11.5 \leq \varepsilon^{57}Fe \leq 2.0$, which show slight enrichment of light isotopes relative to Fe meteorites and the Chinese loess (Web table 2). When plotted as a time series (Fig. 1A), the $\varepsilon^{57}Fe$ values obtained from the Fe-Mn crust show small variations during the period from 6 to 2 million years ago (Ma) but show larger changes starting at 2 Ma. The corresponding time series of $^{206}Pb/^{204}Pb$ ratios from the same Fe-Mn crust is shown in Fig. 1B. It is evident that the time series of $\varepsilon^{57}Fe$ and Pb isotopes are similar, particularly for the part of the crust that developed over the past 2 My. Given the very different nature of these two isotope systems, this similarity is unexpected. The relations between Fe and Pb isotopes are examined further in Fig. 2, where $^{206}Pb/^{204}Pb$ and $^{208}Pb/^{204}Pb$ ratios are compared with $\varepsilon^{57}Fe$. The correlations between $^{206}Pb/^{204}Pb$ and $\varepsilon^{57}Fe$ (Fig. 2A) and $^{208}Pb/^{204}Pb$ and $\varepsilon^{57}Fe$ (Fig. 2B) are strong and are approximate to two linear portions: present day to 2 Ma and from 2 to 6 Ma.

It is important to recall the very different mechanisms by which natural variations in the abundance of Pb and Fe isotopes arise. Lead isotope variations come about through the radioactive decay of $^{232}Th(^{208}Pb)$, $^{235}U(^{207}Pb)$, and $^{238}U(^{206}Pb)$ in environments where U/Pb and Th/U ratios have varied with time (*20*). Moreover, Pb as a heavy and biologically toxic element is known to undergo minimal mass-dependant isotope fractionation in natural physical, chemical, and biological processes. As a result, Pb isotopes vary according to their geological sources. In contrast, Fe is a relatively light element and is essential for life. Isotopes of Fe do not have radiogenic contribution but are expected to undergo mass fractionation in both inorganic and biological processes as a result of thermodynamic and kinetic effects (*21*). The surprising high degree of correlation between Fe and Pb isotopes provides an opportunity to assess possible mechanisms of Fe isotope fractionation.

The overall variation in the $\varepsilon^{57}Fe$ time series obtained from this Fe-Mn crust is more

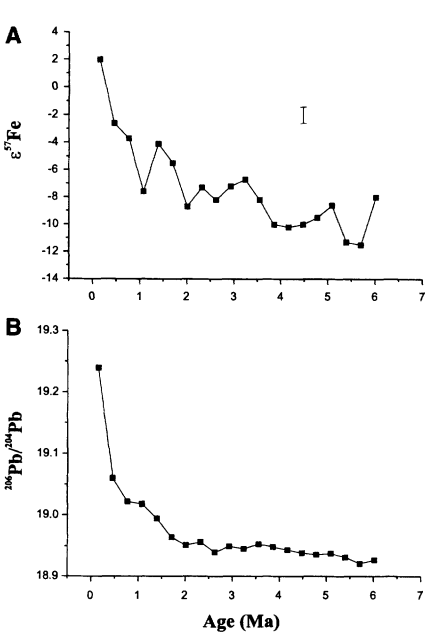

Fig. 1. Time series of **(A)** $\varepsilon^{57}Fe$ and **(B)** $^{206}Pb/^{204}Pb$ in Fe-Mn crust sample BM1969.05, collected from the North Atlantic at 1829-m water depth. Iron isotope variations recorded in the crust over the past 6 My are coherent with those of Pb isotopes, especially for the portion of the crust that developed over the past 2 My. The error bar shown in (A) is at the $\pm 2\sigma$ level. The 2σ error bars for the Pb isotope data are similar in size to the data points and are not shown in the figure.

Department of Earth Sciences, University of Oxford, Parks Road, Oxford, OX1 3PR, UK.

*To whom correspondence should be addressed. E-mail: xiangz@earth.ox.ac.uk

than 10 times the analytical precision. There are several possible explanations for the ε^{57}Fe variation observed, including the following: (i) fractionation of Fe isotopes between seawater and the crust growth surface to a varying degree over time, (ii) redistribution of Fe isotopes in the crust by diagenesis, and (iii) time-dependant variations of Fe isotopes in deep water masses. Because Pb isotopes are not expected to be substantially fractionated by either inorganic or biological processes and because published data for Fe-Mn crusts provide no evidence for diagenetic redistribution of Pb isotopes (*14–16, 22*), the high-degree correlation between Fe and Pb isotopes (Figs. 1 and 2) effectively rules out the first two possibilities as primary causes for the ε^{57}Fe variations. The Fe isotope variations recorded in this crust are therefore interpreted to primarily reflect the time-dependant Fe isotope variations in the North Atlantic Deep Water (NADW) from which the crust grew.

The question now arises as to what is the cause of the Fe isotope variations in seawater. Iron exerts a limiting control on phytoplankton productivity in oceans (*4–8*), and it has been claimed recently that Fe isotope variation in nature is a unique signature of biological processes (*2, 3*). It is therefore intriguing to speculate whether the Fe isotope variations in seawater are a function of oceanic biological productivity. Because Pb is not utilized biologically, the close relations between Fe and Pb isotopes observed in this study imply that there has been no substantial biologically induced mass fractionation of Fe isotopes in seawater since the two isotopic systems became associated, unless the magnitude of such Fe isotope fractionation is in some way correlated with Pb isotope variation in seawater. This possibility appears to be remote. A ready interpretation for the strong correlation between Fe and Pb isotopes is that it reflects a mixing of water bodies with different Fe and Pb isotope compositions. The Fe isotope differences between the water bodies could, in principle, either be inherited from sources that supply both Fe and Pb to the oceans or be the result of biologically induced mass fractionation within the water bodies. However, the almost linear correlation between Fe and Pb isotopes (Fig. 2, A and B) requires that the Fe and Pb isotope compositions in each end-member water body have remained unchanged over more than 2 My. Given the very different nature of these two isotopic systems and the very short residence times for Fe and Pb in seawater, this possibility seems very unlikely.

The Pb isotope history of NADW reconstructed from Fe-Mn crusts requires inputs of Pb through the erosion of two or more continental sources in the North Atlantic area with different Pb isotope compositions (*14–16, 22*). Thus, the correlation shown in Figs. 1 and 2 can be readily explained as that the variations of ε^{57}Fe and Pb isotope ratios are inherited primarily from the continental sources. Whereas the simplest interpretation for the approximate linear relation between Fe and Pb isotopes from 6 to 2 Ma is the mixing of two sources in different proportions over time, the correlation extending from 2 Ma to the present requires an introduction of an additional source for Fe and Pb. This interpretation is further supported by the correlation between Pb isotopes themselves, where the correlation between ^{208}Pb/^{206}Pb and ^{207}Pb/^{206}Pb (Fig. 3A) and ^{208}Pb/^{204}Pb and ^{206}Pb/^{204}Pb (Fig. 3B) is remarkably similar to that observed between Fe and Pb isotopes (Fig. 2). The turnings of the two linear portions in the correlation between Fe and Pb isotopes (Fig. 2) and between Pb isotopes themselves (Fig. 3) are simultaneous. This observation is most readily explained if Fe and Pb in the NADW have come from the same sources without isotope fractionation between their sources and the location of the final hydrogenous precipitation of the Fe-Mn crust itself. However, the close relation between Fe and Pb isotopes observed in this study provides no information about the mechanism of Fe isotope mass fractionation in the source regions.

More detailed discussion about the specific sources of Fe and Pb inputs into NADW and the mechanism of Fe isotope fractionation is not feasible at this stage, because Fe isotopes represent an almost completely unexplored system and there are few data available for comparison. However, the deviation of Fe isotope composition in the Fe-Mn crust from that of the solar system (represented by meteorites) and the upper continental crust (represented by the Chinese loess) is not large (Web tables 1 and 2). Nevertheless, the results demonstrate that Fe isotopes have great potential for paleoceanographic studies. They demonstrate further that Fe isotope variations in seawater are correlated with other better understood parameters such as Pb isotopes. The combined application of Fe and Pb isotope systems to Fe-Mn crusts provides a useful tool to resolve processes affecting Fe isotope fractionation. It shows that biologically induced mass fractionation within seawater is unlikely to be the main cause of the Fe isotope variations observed in this study.

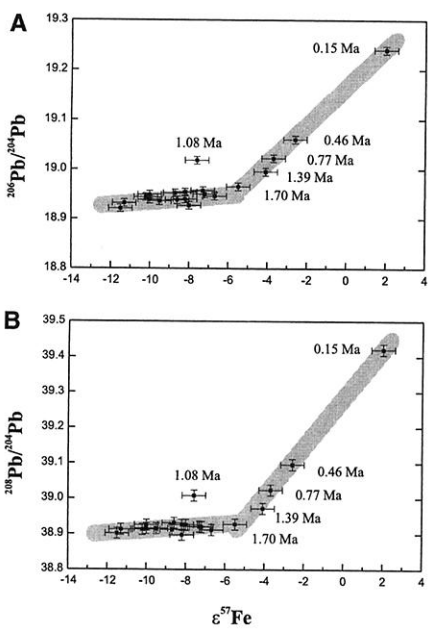

Fig. 2. Comparison of ε^{57}Fe and Pb isotopes in Fe-Mn crust sample BM1969.05. The correlation between Fe and Pb isotopes is high and is time separated at ~1.7 Ma. **(A)** ε^{57}Fe versus ^{206}Pb/^{204}Pb and **(B)** ε^{57}Fe versus ^{208}Pb/^{204}Pb. All error bars shown are at the 2σ level.

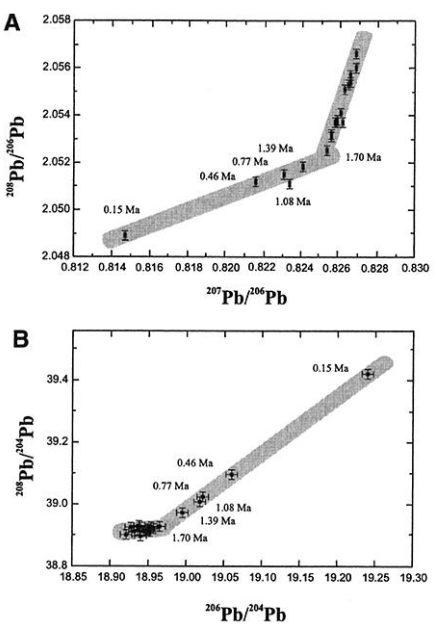

Fig. 3. Correlation between Pb isotope ratios in crust sample BM1969.05. **(A)** ^{208}Pb/^{206}Pb versus ^{207}Pb/^{206}Pb and **(B)** ^{208}Pb/^{204}Pb versus ^{206}Pb/^{204}Pb. All error bars shown are at the 2σ level.

References and Notes

1. N. S. Belshaw, X. K. Zhu, Y. Guo, R. K. O'Nions, *Int. J. Mass Spectrom.* **197**, 191 (2000).
2. B. L. Beard *et al.*, *Science* **285**, 1889 (1999).
3. B. L. Beard and C. M. Johnson, *Geochim. Cosmochim. Acta* **63**, 1653 (1999).
4. J. H. Martin, *Paleoceanography* **5**, 1 (1990).
5. J. H. Martin *et al.*, *Nature* **371**, 123 (1994).
6. H. J. W. de Baar *et al.*, *Nature* **373**, 412 (1995).
7. Z. S. Kolber *et al.*, *Nature* **371**, 145 (1994).
8. D. J. Cooper, A. J. Watson, P. D. Nightingale, *Nature* **383**, 511 (1996).
9. Iron in seawater is largely derived from continental weathering, and the flux into the oceans is a function of climate (*23–25*). The Fe concentration in seawater, in turn, may exert an effect on climate through a control of phytoplankton productivity in the oceans and its utilization of atmospheric CO_2 (*4, 6, 8*).
10. Direct measurement of the Fe isotope composition of seawater is difficult because of the extremely low

abundance of Fe, estimated to be ≤2 nM (*26, 27*), and its very short resident time of $\tau_{Fe} \approx 30$ years (*28*).
11. D. J. Piepgras and D. J. Wasserburg, *Earth Planet. Sci. Lett.* **45**, 223 (1979).
12. F. von Blanckenburg, R. K. O'Nions, N. S. Belshaw, A. J. Gibb, J. R. Hein, *Earth Planet. Sci. Lett.* **141**, 213 (1996).
13. J. N. Christensen, A. N. Halliday, L. V. Godfrey, J. R. Hein, D. K. Rea, *Science* **277**, 913 (1997).
14. K. W. Burton, H. F. Ling, R. K. O'Nions, *Nature* **386**, 382 (1997).
15. R. K. O'Nions, M. Frank, F. von Blanckenburg, H. F. Ling, *Earth Planet. Sci. Lett.* **155**, 15 (1997).
16. B. C. Reynolds, M. Frank, R. K. O'Nions, *Earth Planet. Sci. Lett.* **173**, 381 (1999).
17. Samples of Fe-Mn crust were dissolved in 6 M HCl and then purified by ion-exchange chromatography with 100% yields for Fe. Iron isotope ratios were determined with a Nu Instrument MC-ICPMS, following techniques described in (*1*). The concentration variations between samples and standard were controlled to be less than 20%.
18. X. K. Zhu, R. K. O'Nions, Y. Guo, N. S. Belshaw, D. Rickard, *Chem. Geol.* **163**, 139 (2000).
19. The $^{57}Fe/^{54}Fe$ ratios of samples are expressed in $\varepsilon^{57}Fe$ units according to the following definition:

$$\varepsilon^{57}\mathrm{Fe} = \left(\frac{R_{\mathrm{sample}}}{R_{\mathrm{standard}}} - 1\right) \times 10{,}000$$

where R_{sample} and $R_{standard}$ are the measured $^{57}Fe/^{54}Fe$ ratios for the unknown sample and the IRMM-14 Fe isotope reference standard, respectively. The Fe isotope reference standard IRMM-14 is commercially available and certified by the Institute for Reference Materials and Measurement, European Commission Joint Research Centre.
20. Naturally occurring Pb has four isotopes with masses of 204, 206, 207, and 208 atomic mass units. Of these, ^{206}Pb and ^{207}Pb are produced by the decay of the long-lived isotopes ^{238}U and ^{235}U, and ^{208}Pb is produced by long-lived ^{232}Th. These radiogenic daughters augment the initial abundances of the Pb isotopes in the solar system. The ratios $^{206}Pb/^{204}Pb$, $^{207}Pb/^{204}Pb$, and $^{208}Pb/^{204}Pb$ evolve with time in the natural environment according to time-dependent changes in the ratios of U/Pb and Th/Pb.
21. Iron has four stable isotopes, ^{54}Fe, ^{56}Fe, ^{57}Fe, and ^{58}Fe, with approximate terrestrial abundances of 5.85, 91.75, 2.12, and 0.28%, respectively. The relative abundances of these isotopes are expected to fractionate according to thermodynamic and kinetic effects (*1–3, 29*).
22. W. Abouchami, S. J. G. Galer, A. Koschinsky, *Geochim. Cosmochim. Acta* **63**, 1489 (1999).
23. R. A. Duce and N. W. Tindale, *Mar. Chem.* **36**, 1715 (1991).
24. M. L. Wells, N. M. Price, K. W. Bruland, *Mar. Chem.* **48**, 157 (1995).
25. N. M. Price and F. M. M. Morel, *Met. Ions Biol. Syst.* **35**, 1 (1998).
26. J. Wu and E. A. Boyle, *Anal. Chim. Acta* **367**, 183 (1997).
27. K. S. Johnson, R. M. Gordon, K. H. Coale, *Mar. Chem.* **57**, 137 (1997).
28. J. M. Bewers and P. A. Yeats, *Nature* **268**, 595 (1977).
29. V. B. Polyakov, *Geochim. Cosmochim. Acta* **61**, 4213 (1997).
30. The authors are grateful to N. S. Belshaw for his expertise in mass spectrometry. The constructive comments by two anonymous reviewers are highly appreciated. This work has been supported by a grant from the Natural Environment Research Council.

22 October 1999; accepted 2 February 2000

Modulation of Hurricane Activity in the Gulf of Mexico by the Madden-Julian Oscillation

Eric D. Maloney and Dennis L. Hartmann

The Madden-Julian oscillation (MJO) is a large-scale episodic modulation of tropical winds and precipitation that travels eastward from Asia to America, with a characteristic repeat time of 30 to 60 days. Here it is shown that when MJO wind anomalies in the lower troposphere of the eastern Pacific are westerly, Gulf of Mexico and western Caribbean hurricane genesis is four times more likely than when the MJO winds are easterly. Accurate predictions of the MJO may lead to improved long-range forecasts of tropical cyclone activity.

The Gulf of Mexico coastal regions of the United States have a history of devastating hurricanes and tropical storms (*1*). The deadliest recorded hurricane to hit the United States, the Galveston (Texas) hurricane of 1900, claimed over 8000 lives (*2, 3*). The most intense recorded hurricanes ever to make U.S. landfall—the Florida Keys hurricane of 1935 and Hurricane Camille of 1969—were category 5 hurricanes on the Saffir-Simpson scale (*4, 5*) that ravaged coastal regions of the Gulf of Mexico. The climatologically warm waters of the Gulf of Mexico and the western Caribbean Sea provide an abundant energy source for intense storms during the Atlantic basin hurricane season of May to November (*6*). Increasing our ability to forecast tropical storms and hurricanes has much potential for reducing the loss of life and property associated with these storms.

Here it is shown that the MJO, or tropical intraseasonal oscillation, modulates tropical cyclone activity over the Gulf of Mexico and the western Caribbean Sea. The MJO is characterized by an oscillation in tropical convection and winds at intraseasonal time scales of 30 to 60 days (*7, 8*). Tropical convection, accompanied by wind anomalies, develops over the Indian Ocean and moves eastward toward the Pacific Ocean. Atmospheric circulation anomalies propagate eastward into the eastern Pacific Ocean, where they may be amplified through interactions with convection during the Northern Hemisphere summer season. The MJO causes alternating periods of westerly and easterly wind anomalies (*9*) over the eastern Pacific. Tropical cyclone activity in the Gulf of Mexico appears to vary strongly in association with these intraseasonal wind variations.

This analysis uses wind data at 850 millibars (mb) (about 1400 m above sea level) from National Centers for Environmental Prediction–National Center for Atmospheric Research reanalysis (*10*) during 1949–1997 in pentad (5-day mean) format. Only data from May to November are used, corresponding to the Atlantic basin hurricane season. The reliability of our MJO index in this report is subject to the assumption that the reanalysis product produces realistic winds over the eastern Pacific. A comparison with surface wind data from ship reports (*11*) indicates that the reanalysis wind product agrees reasonably well with observed surface winds in the eastern Pacific. Tropical cyclone records for the Atlantic Ocean are taken from the National Oceanic and Atmospheric Administration (NOAA)/National Weather Service (NWS)/Tropical Prediction Center (*6*).

The principal component (PC) of the first empirical orthogonal function (EOF) for the 850-mb zonal wind is used as a measure of eastern Pacific MJO variability (*12, 13*). The first EOF, or the pattern explaining the maximum amount of temporal variance in the spatial domain of interest, resembles a zonal jet structure over the eastern Pacific, centered near 10°N (*14*). The first PC gives the amplitude of the first EOF as a function of time. This EOF explains 36% of the variance over the eastern Pacific and is closely related to MJO wind variations that emanate from the Indian Ocean and western Pacific regions (*13, 15*). The wind anomalies associated with the leading EOF have been shown to propagate from much farther west, and the EOF amplitude varies with a strong intraseasonal 40- to 50-day rhythm (*13*).

A positive value of the index coincides with westerly wind anomalies over the eastern Pacific Ocean. The average 850-mb wind anomalies for those pentads when the index is 1 SD more or less than zero are plotted in Fig. 1. Only vectors significantly different from zero at the 90% confidence level using a *t* distribution are displayed. The positive composite consists of 325 pentads and the negative composite consists of 322 pentads. Westerly phases are characterized by wind anomalies with cyclonic vorticity (*16*) over the eastern Pacific and the Gulf of Mexico. Tropical cyclone formation is favored in regions of cyclonic low-level relative vorticity (*17, 18*). MJO easterly phases are characterized by anticy-

Department of Atmospheric Sciences, University of Washington, Seattle, WA 98195–1640, USA.